

Second-order transverse magnetic anisotropy induced by disorders in the single-molecule magnet Mn_{12}

Kyungwha Park^{1,2,3,*}, Tunna Baruah^{1,3}, Noam Bernstein¹, and Mark R. Pederson¹

¹Center for Computational Materials Science, Code 6390,

Naval Research Laboratory, Washington DC 20375

²Department of Electrical Engineering and Materials Science Research Center, Howard University, Washington DC 20059

³Department of Physics, Georgetown University, Washington DC 20057

(Dated: November 10, 2018)

For the single-molecule magnet Mn_{12} , Cornia *et al.* recently proposed that solvent molecules may cause the quantum tunneling that requires a lower symmetry than S_4 . However, magnetic quantum tunneling and electron paramagnetic resonance experiments suggested that the proposed theory may not correspond to the measurements. In this regard, we consider positional disorder induced by the solvent molecules and orientational disorder by the methyl groups of a Mn_{12} molecule. We calculate, within density-functional theory, the second-order transverse magnetic anisotropy parameter E and an easy-axis tilting angle θ induced by the positional disorder and the E value by the orientational disorder. We also calculate the local magnetic anisotropy and the local easy axis for each inequivalent Mn site in different environments to investigate their effects on the global E value. We find that the hydrogen bonding between a Mn_{12} molecule and the solvent molecule is crucial to obtain a substantial E value and that the E value increases upon geometry relaxations. Our calculations on relaxed geometries show that the largest calculated E value is 0.016 K and that the largest tilting angle is 0.5° . Our largest E value is comparable to experimental results but larger than Cornia *et al.*'s.

PACS numbers: 75.50.Xx, 75.45.+j, 75.30.Gw, 71.15.Mb

I. INTRODUCTION

Single-molecule magnets (SMMs) are three-dimensional arrays of identical molecules. Each molecule has a large effective spin with a large magnetic anisotropy barrier, and responds to an external magnetic field as a nanoscale, single-domain magnetic particle. As such SMMs are ideal for high-density magnetic storage devices. The most extensively studied SMM is $[\text{Mn}_{12}\text{O}_{12}(\text{CH}_3\text{COO})_{16}(\text{H}_2\text{O})_4] \cdot 2(\text{CH}_3\text{COOH}) \cdot 4(\text{H}_2\text{O})$ (hereafter Mn_{12}).¹ A single molecule of Mn_{12} (Fig. 1) has an effective ground-state spin of $S = 10$ with a magnetic easy axis along the crystal c axis (i.e., z axis), and has S_4 symmetry. Low-temperature magnetization hysteresis loop measurements on Mn_{12} revealed steps at quantized magnetic fields, in which macroscopic quantum tunneling (MQT) occurred between spin-up states and spin-down states through the magnetic anisotropy barrier.^{2,3} Many competing models have been proposed to understand various features of the MQT: fourth-order transverse anisotropy,⁴ thermally assisted quantum tunneling,^{3,5} the Landau-Zener effect,⁶ and dipolar interactions with dynamic hyperfine fields.⁷ However, the observation of quantized steps that are forbidden by the symmetry of a single Mn_{12} molecule remains a long-standing puzzle. It is imperative to fully understand the MQT because higher tunneling rates imply the loss of magnetically stored information, while tunneling is useful in quantum superposition of states crucial to quantum computing⁸.

A general effective single-spin Hamiltonian for SMMs is, to fourth order,

$$\mathcal{H} = DS_z^2 + E(S_x^2 - S_y^2) + C_1S_z^4 + C_2(S_+^4 + S_-^4) + \mathcal{H}' + g\mu_B\vec{B} \cdot \vec{S}, \quad (1)$$

where D is the uniaxial anisotropy parameter, E is the second-order transverse anisotropy parameter, S_z is a spin operator projected onto the easy axis, C_1 and C_2 are the fourfold longitudinal and transverse anisotropy parameters, \mathcal{H}' contains all possible fourth-order terms that break S_4 symmetry, and the last term is the Zeeman interaction. The experimental parameter values are $D = -0.55$ K, $C_1 = -0.00117$ K, and $C_2 = \pm 2.88 \times 10^{-5}$ K.⁹ The MQT is ascribed to the transverse terms in Eq. (1). According to the S_4 symmetry of a Mn_{12} molecule, $E = 0$ and $\mathcal{H}' = 0$ so that the MQT is caused by C_2 alone and is allowed between states whose eigenvalues of S_z differ by integer multiples of 4. However MQT is observed between states that violate this rule. To understand these unexplained tunneling steps, it is necessary to include a lower symmetry than S_4 . Transverse fields caused by internal fields (exchange, dipolar, and hyperfine fields) or field misalignment could induce these steps, but resulting tunneling rates will be too small compared to measured values¹⁰. Thus, a nonzero E value is needed to expedite tunneling assuming that \mathcal{H}' is negligible. So far, two different theories have been proposed in this regard. Chudnovskiy and Garanin¹¹ proposed that possible dislocations in single crystals may provide a broad continuous distribution of E and showed that a broad continuous range of E values is required to explain experiments. Detailed x-ray diffraction studies by Cornia *et al.*¹² suggested that disorder caused by acetic-acid (referred to as HAc) solvent molecules may break the

S_4 symmetry and induce substantial locally varying E values. As discussed in Sec. IIA, such disorder is expected on general grounds. Recently, two completely different experiments^{13,14} have been performed to elucidate the sources of a low symmetry in Mn_{12} . Magnetic quantum tunneling measurements¹³ showed that tunneling splittings (between states whose eigenvalues of S_z do not differ by integer multiples of 4) have much narrower distributions than what the dislocation-induced theory suggested. They also showed that the largest E value for low symmetry molecules is 0.01 K, which is twice larger than what Cornia *et al.*¹² calculated. Electron paramagnetic resonance measurements showed that an upper bound on the E values is 0.014 K,¹⁴ and that some molecules may have an appreciable easy-axis tilt away from the crystal c axis.¹⁵

The two different experiments revealed consistent results that may not be fully explained by either of the two proposed theories. Thus, there is a need for a new theory or a more refined theory that is consistent with the experimental results. In this regard, we investigate the sources of a low symmetry in Mn_{12} within density-functional theory (DFT). Specifically, we consider both positional disorder due to the HAc solvent molecules and orientational disorder caused by methyl-group rotations in Mn_{12} molecules. We find that hydrogen bonding between the Mn_{12} molecules and the solvent molecules is crucial in the second-order transverse anisotropy. We calculate the magnetic anisotropy parameters and the easy-axis tilting angles from the crystal c axis for representative configurations induced by the positional disorder that will be described later. We find that the E value increases upon geometry relaxation, and that there exist relationships, due to symmetry, between the E values for the representative configurations. We also calculate torsional barriers and the magnetic anisotropy parameters for configurations induced by the orientational disorder. Our calculated E values are comparable to the experimental data, while the easy-axis tilting angles remain small. In Sec. II, we describe our method and model for the positional disorder and for the orientational disorder. In Sec. III, we show our results and discuss their consequences. In Sec. IV, we present our conclusion.

II. METHOD AND MODEL

In our DFT calculations¹⁶, we use spin-polarized all-electron Gaussian-orbital-based Naval Research Laboratory Molecular Orbital Library (NRLMOL)¹⁷ within the Perdew-Burke-Ernzerhof (PBE) generalized-gradient approximation (GGA) for the exchange-correlation potential.¹⁸ We consider the following simplified form of Mn_{12} : $[Mn_{12}O_{12}(CH_3COO)_8(HCOO)_8(H_2O)_4] \cdot 2(CH_3COOH)$ where 8 formates ($HCOO$) substituted for 8 acetates (CH_3COO , referred to as Ac) bridging Mn^{4+} ions in the inner cubane and Mn^{3+} ions in the outer crown (Fig. 1). For simplicity, we do not include the water molecules of crystallization. Instead of a periodic structure, we examine an isolated Mn_{12} molecule surrounded by four HAc solvent molecules. The zero-field magnetic anisotropy barrier for the $S = 10$ ground-state manifold does not change much with our simplification nor with attachment of the solvent molecules. The total magnetic moment for the ground state was confirmed to be $20\mu_B$, which is in good agreement with experiment. It is common that the x-ray deduced experimental geometry has underestimated C-H and O-H bond lengths in comparison to standard hydrogen bond lengths, which results in large self-consistent forces on hydrogen atoms as large as an order of 1 hartree/bohr.¹⁹ Therefore, we use as an initial geometry the experimental geometry with hydrogen positions corrected such that all C-H (O-H) bond lengths become 1.1 Å (0.96 Å). Then the initial geometry is self-consistently relaxed using NRLMOL until forces exerted on all atoms are small.

A. Positional disorder

A single Mn_{12} molecule has four HAc solvent molecules, each of which is shared by two neighboring Mn_{12} molecules. From the perspective of the HAc molecule, there are two equivalent ways to place one HAc molecule between two Mn_{12} molecules. That is, the methyl group (CH_3) in HAc can point toward a Mn_{12} molecule or away from it (Fig. 2). In the latter case, there is hydrogen bonding between the oxygen atom O(2) in the Mn_{12} molecule and the oxygen atom O(1) in the solvent molecule (Fig. 1). We refer to this configuration as *head* and the other as *tail* (Fig. 2). There are a total number of 16 ways to place four HAc molecules around a Mn_{12} molecule. Only six of them are inequivalent by symmetry as illustrated in Fig. 2 where n denotes the number of the head configurations. The populations of the six configurations are shown in Table I. The configurations $n = 1$, $n = 2$ trans, $n = 2$ cis, and $n = 3$ break the S_4 symmetry, while $n = 0$ and $n = 4$ preserve the S_4 symmetry. The three configurations, $n = 1$, $n = 2$ cis, and $n = 3$, can cause easy-axis tilts from the crystal c axis which coincides with the z axis, the easy axis without considering the positional disorder.

To examine if the head configuration affects the magnetic anisotropy in the same way as the tail, we consider the following three configurations: (i) two tails only in a twofold symmetric way (trans), (ii) three heads and one tail, and (iii) three heads only. We calculate the D and E values for an initial geometry of each configuration. We find that configuration (i) provides $D = -0.56$ K and $E = 0.00053$ K and that configurations (ii) and (iii) provide the

same parameter values of $D = -0.58$ K and $E = 0.0035$ K. These results imply that the tail configuration does not substantially contribute to the second-order transverse anisotropy. It is thus sufficient to carry out DFT calculations on head-only configurations, which reduces significantly the computation time. Hereafter, unless specified, when we refer to the $n = 1$ configuration, it indicates only one head HAc added to a Mn_{12} molecule without three tail HAc molecules (see the leftmost figure in Fig. 3). The same rule is applied to the rest of the configurations. We also find that both the transverse magnetic anisotropy and the easy-axis tilting angle increase by a factor of 3 upon geometry relaxation.

Especially since we relax an isolated Mn_{12} molecule with solvent instead of a periodic structure, it is worthwhile to check if DFT provides a correct hydrogen bond between two isolated atoms using a simple example system. For this purpose, we carry out DFT calculations for a water dimer. Using its fully relaxed geometry, we obtain the distance between the two oxygen atoms, the O-H-O angle, and its binding energy. They are in excellent agreement with experimental data^{20,21,22} as shown in Table II. This result confirms that DFT captures the hydrogen bonding between Mn_{12} molecules and solvent molecules, and that relaxation of the initial geometries should provide physically refined geometries.

With a well relaxed geometry a second-order single-spin Hamiltonian is calculated considering spin-orbit coupling only.²³ The Hamiltonian has a form of $\sum_{\mu,\nu=x,y,z} \gamma_{\mu\nu} S_\mu S_\nu$. Here $\gamma_{\mu\nu}$ is obtained from the calculated occupied and unoccupied states of the well relaxed geometry and contains the information on the second-order magnetic anisotropy parameters and the principal axes of the magnetic anisotropy. By exploiting symmetry arguments appropriate to the Mn_{12} and the solvent molecules, we can explore all of the six different configurations (Fig. 2) using only the following two configurations. Once the single-spin Hamiltonians for the $n = 0$ and $n = 1$ configurations are calculated, those for the remaining four configurations can be obtained by rotations of coordinates. For instance, we can describe the Hamiltonian for $n = 2$ trans (cis), $\mathcal{H}[n = 2]$, in terms of those for $n = 0$, $\mathcal{H}[n = 0]$, and $n = 1$, $\mathcal{H}[n = 1]$, using a rotation matrix R (see Fig. 3).

$$\mathcal{H}[n = 0] \equiv \sum_{\mu,\nu=x,y,z} \gamma_{\mu\nu}^{(0)} S_\mu S_\nu, \quad \mathcal{H}[n = 1] \equiv \sum_{\mu,\nu=x,y,z} \gamma_{\mu\nu}^{(1)} S_\mu S_\nu, \quad (2)$$

$$\begin{aligned} \mathcal{H}[n = 2] &= \sum_{\mu,\nu=x,y,z} \gamma_{\mu\nu}^{(1)} [S_\mu S_\nu + R(S_\mu)R(S_\nu)] - \sum_{\mu,\nu=x,y,z} \gamma_{\mu\nu}^{(0)} S_\mu S_\nu \\ &\equiv \sum_{\mu,\nu=x,y,z} \gamma_{\mu\nu}^{(2t),(2c)} S_\mu S_\nu \end{aligned} \quad (3)$$

$$\gamma_{xy}^{(2t)} = 2\gamma_{xy}^{(1)}, \quad \gamma_{xz}^{(2t)} = 0, \quad \gamma_{yz}^{(2t)} = 0, \quad (4)$$

$$\gamma_{xy}^{(2c)} = 0, \quad \gamma_{xz}^{(2c)} = \gamma_{xz}^{(1)} - \gamma_{yz}^{(1)}, \quad \gamma_{yz}^{(2c)} = \gamma_{xz}^{(1)} + \gamma_{yz}^{(1)} \quad (5)$$

$$\gamma_{xy}^{(3)} = \gamma_{xy}^{(1)}, \quad \gamma_{xz}^{(3)} = -\gamma_{yz}^{(1)}, \quad \gamma_{yz}^{(3)} = \gamma_{xz}^{(1)} \quad (6)$$

where $\gamma^{(2t)}$, $\gamma^{(2c)}$, and $\gamma^{(3)}$ stand for the γ matrices for the $n = 2$ trans, $n = 2$ cis, and $n = 3$ configurations, respectively. Here we show only the off-diagonal elements of the γ matrices. Since $n = 0$ has the S_4 symmetry, $\gamma_{xy}^{(0)} = \gamma_{xz}^{(0)} = \gamma_{yz}^{(0)} = 0$. We have also verified this numerically.

B. Orientational disorder

The methyl group in Ac can rotate about the C-C single bond. During the rotation, the energy of the methyl group will change. The difference between the maximum and the minimum energy is called a torsional barrier. For an isolated Ac molecule, the torsional barrier is calculated to be about 320 K, which is comparable to the thermal energy at room temperature. So it is interesting to examine if the orientational disorder caused by rotations of the methyl groups can induce the appreciable second-order transverse anisotropy. We consider rotations of the methyl groups in a Mn_{12} molecule, and there are three inequivalent Ac sites. The methyl groups in the Ac molecules bridging the inner Mn ions and the outer Mn ions will have less freedom to rotate and therefore a smaller effect on the transverse anisotropy. The methyl groups of type A (Fig. 1) are close to the HAc solvent molecules so they also have less freedom to rotate. Thus we rotate the methyl groups of type B (in the Ac molecules that are free from the HAc molecules) with the methyl groups of type A fixed. In this study, we do not allow solvent-induced symmetry breaking and do not consider geometry relaxation induced by methyl rotations. We consider an initial geometry of the $n = 4$ configuration with several methyl groups of type B rotated, and calculate the torsional barriers and the magnetic anisotropy parameters.

III. RESULTS

A. Positional disorder

The well relaxed geometry for the $n = 0$ configuration gives rise to $D = -0.54$ K and $E = 0$. The well relaxed geometry for the $n = 1$ configuration provides $D = -0.54$ K, $E = 0.008$ K, and the easy-axis tilting angle $\theta = 0.4^\circ$. Using this result and Eqs. (2)-(6), we calculate D , E , and θ for the $n = 2$ trans, $n = 2$ cis, $n = 3$, and $n = 4$ configurations (Table I). The D value does not vary much among the different configurations. (Note that $D = -0.55$ K without solvent molecules.²³) The E value for $n = 1$ is the same as that for $n = 3$ and is one half of that for $n = 2$ trans. The E value for $n = 2$ cis is two orders of magnitude smaller than that for $n = 1$. The largest E value arises from $n = 2$ trans, while the largest θ comes from $n = 2$ cis. The E values for the low-symmetry configurations are determined by all the off-diagonal elements of the $\gamma^{(1)}$ matrix, while the easy-axis tilts are due only to the nonzero $\gamma_{xz}^{(1)}$ and $\gamma_{yz}^{(1)}$ values [Eqs. (2)-(6)]. For the positional disorder, the magnitudes of all the off-diagonal elements of the $\gamma^{(1)}$ matrix are very small compared to those of the diagonal elements. Therefore, there is no appreciable easy-axis tilt and there is a relation between the E values for different configurations. The $n = 2$ cis configuration does not have a significant contribution to the transverse anisotropy. If the magnitudes of the off-diagonal elements are significant, there is a substantial easy-axis tilt and the E values for the distinctive configurations are not correlated. Additionally, the E value for $n = 2$ cis has the same order of magnitude as those for the other low-symmetry configurations. This occurs when extra electrons are donated to a Mn_{12} molecule since the locations of the extra electrons are intrinsically dependent on donor locations.²⁴ In comparison to Cornia *et al.*'s results,¹² our calculated E values are larger by a factor of 3 and our easy-axis tilting angle is almost the same. In comparison to the experimental data,^{13,14,15} our largest E value is in good agreement but our largest easy-axis tilting angle is smaller than 1° .

To examine the effect of the positional disorder on the local magnetic anisotropy, we calculate the single-ion anisotropy parameters²⁵ and the local magnetic easy-axis tilts for the three inequivalent Mn sites in two different environments. These three sites are the cubane Mn^{4+} ion (at site c in Fig. 1) and two Mn^{3+} ions (at sites r and b in Fig. 1). The two environments correspond to (i) the head and (ii) tail configurations. For the environments (i) and (ii) we use a well relaxed $n = 2$ trans (two heads and two tails) geometry. Before showing our results, we describe our method. The lowest-order energy shift Δ_2 due to spin-orbit coupling V_{LS} is²³

$$\Delta_2 = \sum_{\sigma, \sigma'} \sum_{ij} \frac{\langle \psi_{i\sigma} | V_{LS} | \psi_{j\sigma'} \rangle \langle \psi_{j\sigma'} | V_{LS} | \psi_{i\sigma} \rangle}{\epsilon_{i\sigma} - \epsilon_{j\sigma'}}, \quad (7)$$

where $\epsilon_{i\sigma}$ ($\epsilon_{j\sigma'}$) denotes the energy of the i th occupied (j th unoccupied) unperturbed state whose wavefunction is $|\psi_{i\sigma}\rangle$ ($|\psi_{j\sigma'}\rangle$). The first sum runs over spin-up and spin-down states and the second sum over all occupied and unoccupied states. A wavefunction of the system is expanded in a sum of contributions associated with each atom, $|\psi_{i\sigma}\rangle = \sum_{\alpha} |\psi_{i\sigma}^{\alpha}\rangle$ and $|\psi_{j\sigma'}\rangle = \sum_{\alpha} |\psi_{j\sigma'}^{\alpha}\rangle$, where the sums run over all atoms. Thus, Δ_2 can be written in terms of projected terms onto each atom and mixed terms between different atoms as follows:

$$\Delta_2 = \sum_{\alpha} \sum_{\sigma, \sigma'} \sum_{ij} \frac{\langle \psi_{i\sigma}^{\alpha} | V_{LS} | \psi_{j\sigma'}^{\alpha} \rangle \langle \psi_{j\sigma'}^{\alpha} | V_{LS} | \psi_{i\sigma}^{\alpha} \rangle}{\epsilon_{i\sigma} - \epsilon_{j\sigma'}} + \sum_{\alpha\beta\gamma\delta} \sum_{\sigma, \sigma'} \sum_{ij} \frac{\langle \psi_{i\sigma}^{\alpha} | V_{LS} | \psi_{j\sigma'}^{\beta} \rangle \langle \psi_{j\sigma'}^{\gamma} | V_{LS} | \psi_{i\sigma}^{\delta} \rangle}{\epsilon_{i\sigma} - \epsilon_{j\sigma'}} \quad (8)$$

where the first sum of the mixed term runs over all cases where at least two of the indices $\alpha\beta\gamma\delta$ are different. Based on the assumption that the contributions associated with each atom, $|\psi_{i\sigma}^{\alpha}\rangle$, have small interatomic overlap, which is the case for Mn_{12} , the mixed terms are expected to be negligible. This is true considering the relative magnitude of the Coulomb potential near an atom compared to the interstitial region. Thus Δ_2 is approximately equal to the tensor sum of the projected terms onto all atoms, the first term in Eq. (8). Regardless of the types of the environments, a cubane Mn^{4+} ion has the local easy axis almost in the xy plane (the local E value is of the same order as the local D value) and the two crown Mn^{3+} ions have the local easy axis close to the z axis. Therefore the Mn^{3+} ions contribute most of the total magnetic anisotropy. Since the Mn^{4+} ions are far away from the solvent molecules, the local E value for the head configuration is the same as that for the tail. For the two inequivalent Mn^{3+} ions, the local E value is sensitive to the environments, while the local D value and the local easy-axis tilting angles are not sensitive to them. Especially for the Mn^{3+} ions of type b, the local E value for the tail configuration is an order of magnitude smaller than that for the head. This large difference in the local E values of the head and tail configurations leads to the large global E value.

We also calculate tunnel splitting $\Delta_{-10,4}$ between $M_s = -10$ and $M_s = 4$, where M_s is an eigenvalue of S_z (Table I) for the six distinctive configurations perturbatively and by exact diagonalization. We use our calculated values for D and E and the experimental values⁹ for C_1 and C_2 . The tunneling between $M_s = -10$ and $M_s = 4$ is allowed due to

the nonzero second-order transverse anisotropy but the magnitude of the tunnel splitting is mostly governed by the fourth-order transverse anisotropy. So the tunnel splitting is very dependent on the C_2 value but less on the E value. As shown in Table I, if we reduce the C_2 value by one half from the experimental value while keeping other parameter values constant, the tunnel splitting is reduced by an order of magnitude. Thus, the experimental value of $\Delta_{-10,4}[10]$ may not be a good indicator of the magnitude of the E value.

B. Orientational disorder

When the four methyl groups of type B are rotated relative to those of type A in the $n = 4$ configuration, we find that there are at least four local energy minima at the rotation angles of -10° , -25° , 0° , and 30° where 0° denotes the experimental geometry. Since the four methyl groups are rotated simultaneously, we have to divide by 4 to obtain the torsional barriers per methyl group for each rotation angle. As shown in Table IV, the torsional barriers at the three nonzero rotation angles are comparable to the thermal energy at room temperature. So we consider the three twofold symmetric configurations, which correspond to $n = 4$ with two methyl groups of type B across from each other rotated by -10° , -25° , and 30° . Our calculations show that the E values for all three angles are on the order of 10^{-4} K, which is much smaller than those due to the positional disorder (Table IV).

IV. CONCLUSION

Considering the solvent positional disorder and the orientational disorder of the methyl groups in the Mn_{12} molecules, we investigated, within density-functional theory, the sources of the second-order transverse magnetic anisotropy in Mn_{12} . We found that only hydrogen-bonded solvent molecules contribute to the symmetry-breaking transverse anisotropy, and that geometry relaxation is necessary from the standpoint of quantitative prediction. For the positional disorder, the large E value is due to the large difference between the local E values of the two different environments (the head and tail configurations). There are no significant easy-axis tilts from the z axis for the low-symmetry configurations. Accordingly, the E values for the different configurations are correlated. The orientational disorder contributes to the E value much less than the positional disorder. Our largest calculated E value from the positional disorder quantitatively agrees with the experimental data. However unresolved issues remain. That is, the experimental E values suggest a *continuous* distribution rather than a discrete distribution that is predicted by the positional disorder.

Acknowledgments

This work was supported in part by the ONR (Grant No. N000140211045), the NRL, the DoD HPCMPO and CHSSI program, and the W.M. Keck Foundation (K.P.).

-
- * Electronic address: park@dave.nrl.navy.mil
- ¹ T. Lis, Acta Crystallogr. B **36**, 2042 (1980).
 - ² R. Sessoli, D. Gatteschi, A. Caneschi, and M.A. Novak, Nature (London) **365**, 141 (1993).
 - ³ J. R. Friedman, M. P. Sarachik, J. Tejada, and R. Ziolo, Phys. Rev. Lett. **76**, 3830 (1996).
 - ⁴ J. Villain, F. Hartman-Boutron, R. Sessoli, and A. Rettori, Europhys. Lett. **27**, 159 (1994); F. Hartmann-Boutron, P. Politi, and J. Villain, Int. J. Mod. Phys. B **10**, 2577 (1996); A. Fort, A. Rettori, J. Villain, D. Gatteschi, and R. Sessoli, Phys. Rev. Lett. **80**, 612 (1998).
 - ⁵ D. A. Garanin and E. M. Chudnovsky, Phys. Rev. B **56**, 11 102 (1997); F. Luis, J. Bartolomé, and F. Fernández, *ibid.* **57**, 505 (1998); M. N. Leuenberger and D. Loss, Phys. Rev. B **61**, 1286 (2000).
 - ⁶ H. De Raedt, S. Miyashita, K. Saito, D. García-Pablos, and N. García, Phys. Rev. B **56**, 11 761 (1997); V. V. Dobrovitsky and A. K. Zvezdin, Europhys. Lett. **38**, 377 (1997); , Phys. Rev. B **61**, 12 200 (2000).
 - ⁷ N. V. Prokof'ev and P. C. E. Stamp, Phys. Rev. Lett. **80**, 5794 (1998); W. Wernsdorfer, T. Ohm, C. Sangregorio, R. Sessoli, D. Mailly, and C. Paulsen, *ibid.* **82**, 3903 (1999).
 - ⁸ M. N. Leuenberger and D. Loss, Nature (London) **410**, 789 (2001).
 - ⁹ A. L. Barra, D. Gatteschi, and R. Sessoli, Phys. Rev. B **56**, 8192 (1997).
 - ¹⁰ K. M. Mertes, Y. Suzuki, M. P. Sarachik, Y. Paltiel, H. Shtrikman, E. Zeldov, E. Rumberger, D. N. Hendrickson, G. Christou, Phys. Rev. Lett. **87**, 227205 (2001).

- ¹¹ E. M. Chudnovsky and D. A. Garanin, Phys. Rev. Lett. **87**, 187203 (2001); Phys. Rev. B **65**, 094423 (2002).
- ¹² A. Cornia, R. Sessoli, L. Sorace, D. Gatteschi, A. L. Barra, and C. Daignebonne, Phys. Rev. Lett. **89**, 257201 (2002).
- ¹³ E. del Barco, A. D. Kent, E. M. Rumberger, D. N. Hendrickson, and G. Christou, Europhys. Lett. **60**, 768 (2002); E. del Barco, A. D. Kent, E. M. Rumberger, D. N. Hendrickson, and G. Christou, Phys. Rev. Lett. **91**, 047203 (2003).
- ¹⁴ S. Hill, R. S. Edwards, S. I. Jones, N. S. Dalal, and J. M. North, Phys. Rev. Lett. **90**, 217204 (2003).
- ¹⁵ R. S. Edwards, S. Hill, S. Maccagnano, N. S. Dalal, and J. M. North (unpublished).
- ¹⁶ W. Kohn and L. J. Sham, Phys. Rev. **140**, A1133 (1965).
- ¹⁷ M. R. Pederson and K. A. Jackson, Phys. Rev. B **41**, 7453 (1990); K. A. Jackson and M. R. Pederson, *ibid.* **42**, 3276 (1990); D. V. Porezag, Ph.D. thesis, Chemnitz Technical Institute, 1997.
- ¹⁸ J. P. Perdew, K. Burke, and M. Ernzerhof, Phys. Rev. Lett. **77**, 3865 (1996).
- ¹⁹ K. Park, M. R. Pederson, S. L. Richardson, N. Aliaga-Alcalde, and G. Christou, Phys. Rev. B **68**, 020405(R) (2003).
- ²⁰ J. A. Odutola and T. R. Dyke, J. Chem. Phys. **72**, 5062 (1980).
- ²¹ L. A. Curtiss, D. L. Frurip, and M. Blander, J. Chem. Phys. **71**, 2703 (1979).
- ²² R. M. Bentwood, A. J. Barnes, and W. J. O. Thomas, J. Mol. Spectrosc. **84**, 391 (1980).
- ²³ M. R. Pederson and S. N. Khanna, Phys. Rev. B **60**, 9566 (1999).
- ²⁴ K. Park, T. Baruah, and M. R. Pederson (unpublished).
- ²⁵ T. Baruah and M. R. Pederson, Chem. Phys. Lett. **360**, 144 (2002).

TABLE I: Populations, calculated magnetic anisotropy parameters (D and E), easy-axis tilting angles θ , and tunnel splittings between $M_s = -10$ and $M_s = 4$, $\Delta_{-10,4}$, for six distinctive configurations of an isolated Mn_{12} molecule with four HAc solvent molecules. See Fig. 2. For $\Delta_{-10,4}[\text{A}]$, we use $C_1 = -0.00117$ K and $C_2 = 2.88 \times 10^{-5}$ K.⁹ For $\Delta_{-10,4}[\text{B}]$, we use $C_1 = -0.00117$ K and $C_2 = 1.44 \times 10^{-5}$ K.

configuration	population	D (K)	E (K)	θ (degree)	$\Delta_{-10,4}[\text{A}]$	$\Delta_{-10,4}[\text{B}]$
$n = 0$	$\frac{1}{16}$	-0.54	0	0	0	0
$n = 4$	$\frac{1}{16}$	-0.56	0	0	0	0
$n = 1$	$\frac{4}{16}$	-0.54	0.008	0.4	7.0×10^{-7}	7.8×10^{-8}
$n = 2$ cis	$\frac{4}{16}$	-0.55	0.00002	0.5	1.8×10^{-9}	4.4×10^{-11}
$n = 2$ trans	$\frac{2}{16}$	-0.55	0.016	0	1.0×10^{-6}	9.3×10^{-8}
$n = 3$	$\frac{4}{16}$	-0.55	0.008	0.4	6.7×10^{-7}	8.1×10^{-8}

TABLE II: DFT calculated hydrogen bond length between the two oxygen atoms $R(\text{O-O})$, the bond angle (O-H-O) , and its binding energy for a water dimer in comparison to experimental data.^{20,21,22}

	$R(\text{O-O})$ (Å)	$\angle(\text{O-H-O})$ (degree)	binding energy (eV)
DFT	2.906	174	0.223
Exp.	2.946 [20]	174 [21]	0.232 ± 0.030 [22]

TABLE III: Calculated local magnetic anisotropy parameters (D and E), local easy-axis tilting angles δ , and local anisotropy barriers for the three inequivalent Mn sites in different environments. Here "c", "r", and "b" stand for the three sites shown in Fig. 1. "head" and "tail" denote the head and tail configurations of the HAc solvent molecules.

site	D (K)	E (K)	δ (degree)	barrier (K)
$\text{Mn}^{4+}(\text{c, head})$	-0.50	0.18	101.5	0.72
$\text{Mn}^{4+}(\text{c, tail})$	-0.52	0.18	88.4	0.77
$\text{Mn}^{3+}(\text{r, head})$	-2.44	0.037	11.8	9.6
$\text{Mn}^{3+}(\text{r, tail})$	-2.47	0.016	11.4	9.8
$\text{Mn}^{3+}(\text{b, head})$	-2.54	0.23	34.5	9.2
$\text{Mn}^{3+}(\text{b, tail})$	-2.65	0.036	36.2	10.4

TABLE IV: Calculated torsional barriers per methyl group and magnetic anisotropy parameters due to rotations of two methyl groups of type B (Fig. 1) across from each other in the $n = 4$ configuration. The barriers are calculated from the closest local minimum configurations.

rotation angle (degree)	torsional barrier (K)	D (K)	E (K)
-10	316	-0.57	0.00009
-25	308	-0.57	0.0002
30	60	-0.57	0.0001

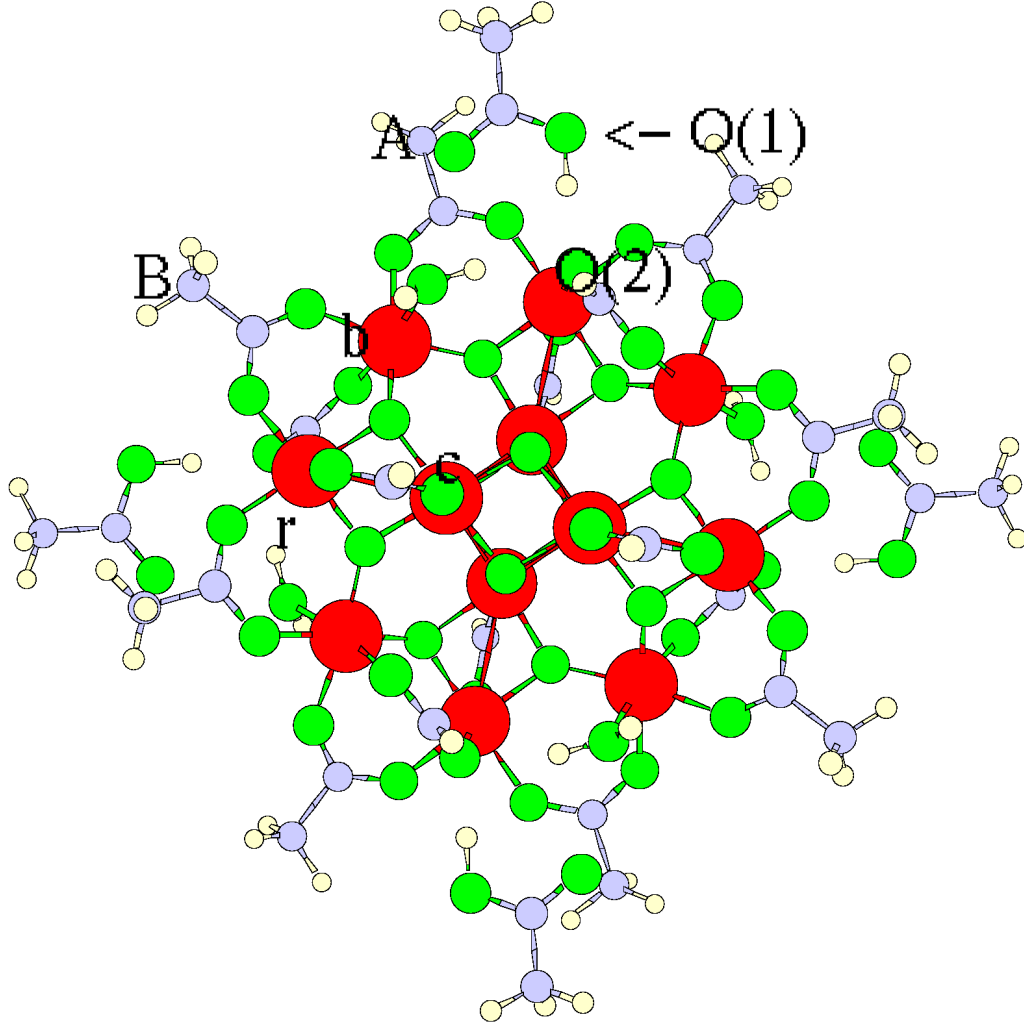


FIG. 1: A single Mn_{12} molecule surrounded by four HAc solvent molecules, $[\text{Mn}_{12}\text{O}_{12}(\text{CH}_3\text{COO})_8(\text{HCOO})_8(\text{H}_2\text{O})_4]4(\text{CH}_3\text{COOH})$. The sizes of atoms decrease in the order of Mn, O, C, and H. The four inner cubane Mn^{4+} ions ($S = 3/2$) are ferromagnetically coupled to each other and the eight outer crown Mn^{3+} ($S = 2$) ions are ferromagnetically coupled. The Mn spins in the crown are antiparallel to those in the cubane, which results in the total effective ground-state spin of $S = 10$. The easy axis of the molecule is normal to the page. Two inequivalent acetates are labeled as “A” and “B”. The hydrogen bond is formed between oxygen atoms O(1) and O(2).

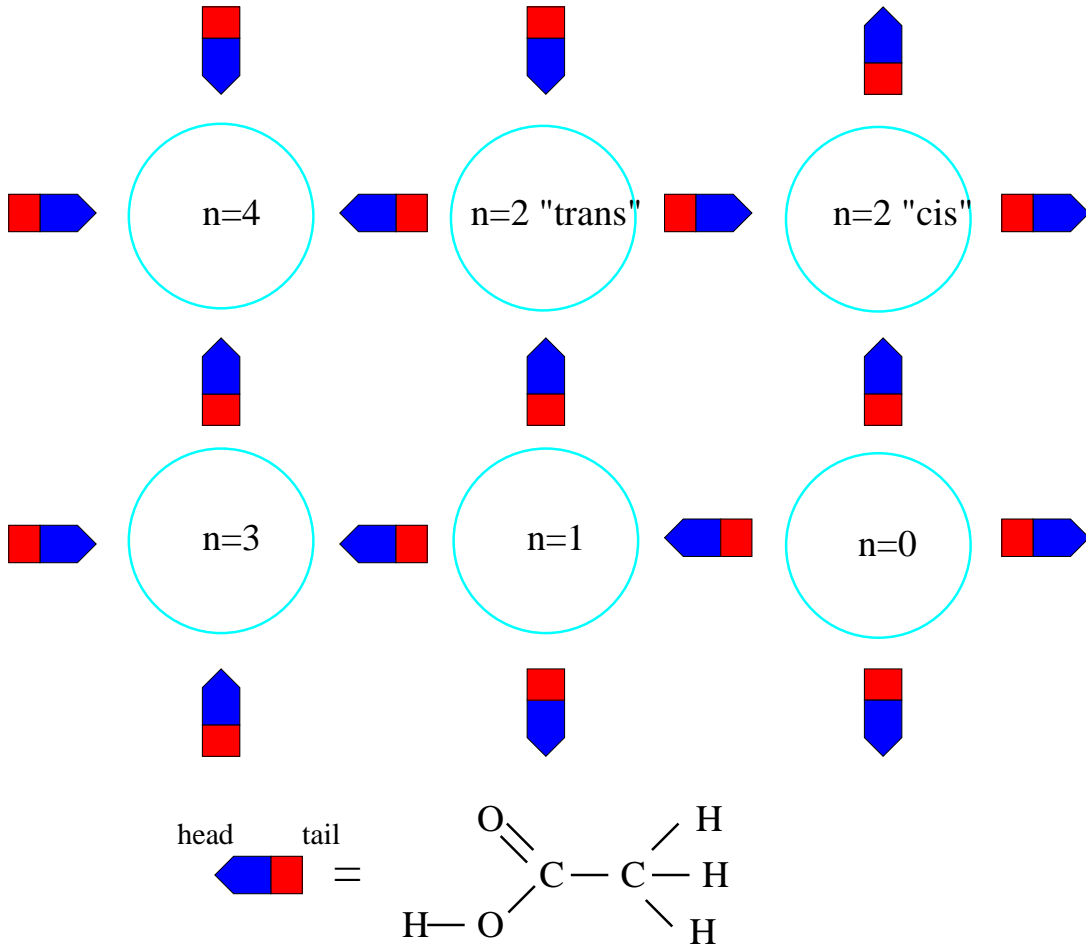


FIG. 2: Six distinct configurations of a Mn_{12} molecule with four HAc solvent molecules. The circles represent Mn_{12} molecules. n is the number of HAc molecules whose heads point into a Mn_{12} molecule. From the top leftmost, clockwise, the symmetry of each configuration is S_4 , C_2 , C_1 , S_4 , C_1 , and C_1 .

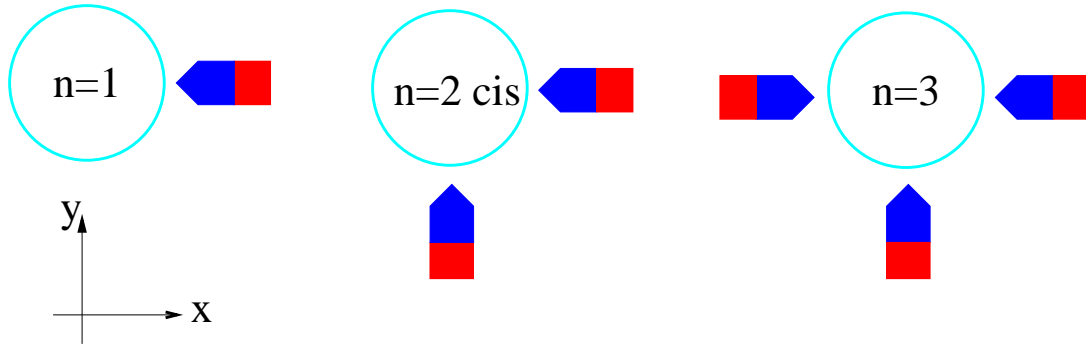


FIG. 3: Three head-only configurations used for Eqs. (4)-(6).